Frontiers in Mechanochemistry and Mechanical Alloying

INCOME2008
1-4 December, 2008

SYNTHESIS AND CHARACTERIZATION OF NANOCRYSTALLINE CARBIDES BY REACTION MILLING

D. Chaira[1], B.K. Mishra[2ξ], S. Sangal[3]
[1]Department of Metallurgical & Materials Engineering, National Institute of Technology Rourkela, Orissa, India
[2] CSIR-Institute of Minerals and Materials Technology, Bhubaneswar, Orissa, India
[3]Department of Materials & Metallurgical Engineering, Indian Institute of Technology Kanpur, U.P, India

Keywords: Dual drive planetary mill; Nanocrystalline carbides; Cementite; Silicon carbide; Titanium carbide; Reaction milling

Abstract

Nanocrystalline cementite, silicon carbide and titanium carbide powders were prepared from elemental constituent powder particles by reaction milling. A high energy dual drive planetary mill has been fabricated for the synthesis of carbides. The strong collision energy field of the dual drive planetary mill reduced the carbide formation time as compared to earlier reported studies. Forty hours is required to produce nanocrystalline cementite and silicon carbide powder. Whereas only 10 hours is required to produce titanium carbide powder, because self propagating reaction takes place between Ti and graphite during milling. The morphology of powders and evolution of different phases were studied by X-ray diffraction (XRD), scanning electron microscopy (SEM) and transmission electron microscopy (TEM).

Introduction

Carbides possess unusual properties that make them desirable and useful engineering materials for many industrial applications. One important property of the carbides is their chemical stability at room temperature—they degrade slowly when subjected to highly concentrated acidic media. In fact, carbides are unique in that they combine the characteristic properties of metals and ceramics. Therefore, these materials are hard; resist wear; possess good thermal conductivity and oxidation resistance. For these reasons, carbides are used in a wide range of applications from refractory bricks to cutting tools. A systematic investigation is made with respect to the preparation in bulk and characterization of carbides. Three industrially important carbides viz., cementite (Fe_3C), silicon carbide (SiC) and titanium carbide (TiC) are studied. These are synthesized up to 1 kg in batch from their corresponding elemental constituents by reaction milling in a specially built dual drive planetary mill.

Cementite is a major constituent of iron-carbon alloys. These alloys attracted attention due to their low cost and high strength applications. Up until now, the interest in fabrication of Fe-C alloy had been focused only on low carbon concentration whereas high carbon concentrations were treated only on a limited scale. The main reason is that even today issues relating to interaction between different phases, effect of alloying element, etc., are not resolved, e.g. cementite is one of the most important phases in steel, which is responsible to a large extent for its mechanical property. It also holds a lot of promise as a dispersoid for the synthesis of composites. The understanding of mechanical and physical properties of steel vis-à-vis cementite is not well established. Since cementite is hard and brittle at room temperature and meta-stable at all temperatures, it is difficult to synthesize and isolate as single-phase material under ordinary processing conditions. Cementite has no direct industrial application but it draws a lot of theoretical interest, as it is mainly responsible for the mechanical property of steel.

Unlike cementite, silicon carbide (SiC) has many direct industrial applications. It is used in electronic devices that are particularly used at high temperatures. This is due to its high temperature electrical properties, high breakdown voltage and high electron mobility. It is also used in various types of high temperature applications such as heating elements and refractory material for furnaces due to its high fracture strength, excellent wear and creep resistance, high resistance to corrosion, good thermal conductivity and relatively low coefficient of thermal expansion. It is also a good filler material due to its thermal and chemical stability. This is valid both during synthesis and under severe service conditions.

Titanium carbide (TiC) is a material of commercial interest because it possesses a number of desirable properties. It is one of the hardest known metal carbides (Ye, L. L. *et al.,* 1995) and it exhibits excellent thermal stability and has a very high melting temperature of approximately 3100°C. It also displays relatively high thermal and electrical conductivity. In high temperature applications, higher thermal conductivity of TiC is an advantage as it results in lower thermal gradients, which reduces thermal stresses and cracking that makes it suitable for high-speed cutting tool applications. Similarly, good electrical conductivity of TiC makes it suitable for electrical discharge machining. Additionally, TiC has a low density, which is desirable for lightweight applications. It also exhibits excellent chemical stability, which is important for cutting tool applications, as chemical stability reduces the chemical interaction between the cutting tool and the work piece.

The main aim of this work is to gain a better understanding of the reaction milling process and its products—Fe_3C, SiC and TiC. The results of this work shall add to the fundamental understanding of the reaction milling process to synthesize carbides, which in turn can be utilized to pilot the process as a commercial option for bulk synthesis of carbides.

ξ email : abcl_mishra@yahoo.com

Experimental

Mill Design

The dual drive planetary mill developed specifically for the synthesis of nanocrystalline carbides has a rotating shaft that sweeps a circle of diameter 750 mm. The two steel jars of 135 mm diameter (2500 ml each) rotate about their own axes around the common axis of the main shaft. The planetary mill is powered by two motors. A 5 HP motor works on the main rotating shaft and 3 HP motor drives the jars. The rotating speed of both motors can be varied independently and continuously by a frequency controller. This mill design follows closely the patented design of Rajamani *et al.* (2000) with several minor modifications to improve its performance and suit to the local conditions. Details of mill design and mill mechanics are available (Chaira et al. 2007). Figure 1 shows the dual drive planetary mill.

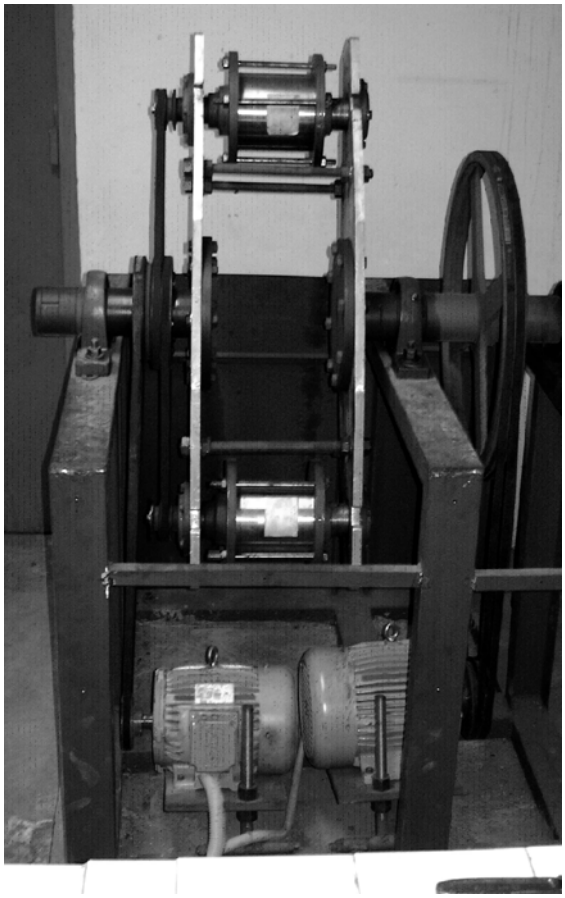

Figure 1. Dual drive planetary mill

Synthesis of Nanocrystalline Cementite Powder

For the synthesis of cementite powder, iron and graphite powder with 99% purity were used in stoichiomatric ratio. Milling experiments were conducted in two jars each containing 250 grams of powder and 2.5 kg of steel balls for times varying from 6 hours to 50 hours. Sample of milled product was characterized by using X-ray diffraction, SEM and TEM.

Synthesis of Nanocrystalline Silicon Carbide Powder

Silicon and graphite powder with 99.5 and 99% purity were taken as starting materials. Powders were mixed in 1:1 atomic ratio and milling was carried out for 40-hours in two jars-each containing 125 gm powder and 2.5 kg steel balls. Steel balls of diameter 6 and 12 mm were used for milling to study the effect of ball size.

Synthesis of Nanocrystalline Titanium Carbide Powder

In one jar titanium and graphite and in the other jar titanium and activated carbon were taken for the synthesis of TiC powder. Powders were taken in 1:1 atomic ratio. Here only 50 gm powder and 1 kg steel balls were taken for grinding. Milling was carried out for a period of 10 hours.

Results and Discussions

Characterization of Cementite Powder

In order to determine the phase change of the particle mixtures during the reaction milling process, a small sample of milled product was collected at regular intervals for X-ray diffraction analysis. The XRD patterns of the end product (as-milled powder) are shown in Fig. 2 for different intervals of milling time.

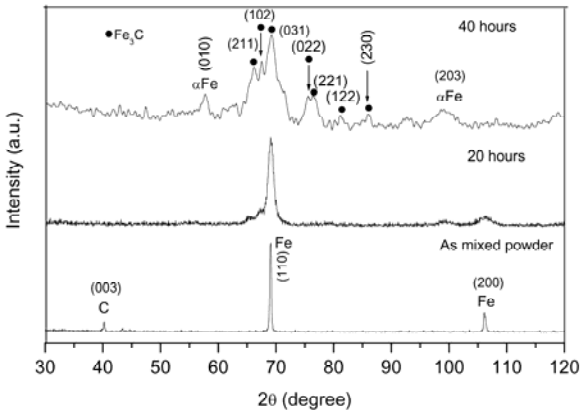

Figure 2. XRD patterns of Fe-6.7 wt% graphite powder at selected milling times

Several interesting observations could be made from Fig. 2. First, the graphite peak disappeared after about 20 hours of milling. This is a general observation in this study, which may be due to amorphization of graphite during milling. Second, it was observed that the peak positions of iron shift to a lower angle with increasing milling time. The shift of the iron peaks position to the lower angle means that carbon atoms form a solid solution with iron. It was also observed that iron peaks broaden and their integrated intensity decreases with milling time. This suggests the accumulation of lattice strain and reduction of crystal size. Finally, peak corresponding to cementite is observed along with elemental iron and ferrite after 40-hours of grinding. Milling experiments beyond 40 hours were also done. However, no change in the intensity of the carbide peaks was

observed. Therefore, it is concluded that 40 hours was the optimum milling time. In comparison, Umemoto *et al.* (2004) produced bulk cementite from elemental iron and graphite powder by mechanical alloying in horizontal ball mill after 100 hours of milling. Wang and Campbell *et al.* (1995) also milled iron and graphite powder mixture in argon atmosphere up to 210 hours to produce cementite powder.

The SEM was used to study changes in shape and size of the milled powder during different stages of the reaction milling process. Figure 3 shows the SEM images at different milling times. Initially, up to 2 hours, the starting elemental particles of iron and graphite agglomerate to form composite particles of larger diameter. These particles undergo cold welding by binding to each other under stress. As a result, their morphology changes from an irregular to flaky shape. In the intermediate stage, between 6 to 20 hours, when reaction milling is likely to occur, fragmentation of particles and atomic diffusion between particles also occur. Towards the end, between 20 to 40-hours, the powder particles are subjected to extreme conditions in terms of size reduction and mechanical activation. As a result, most particles are less than 10 micrometers and are visibly spherical.

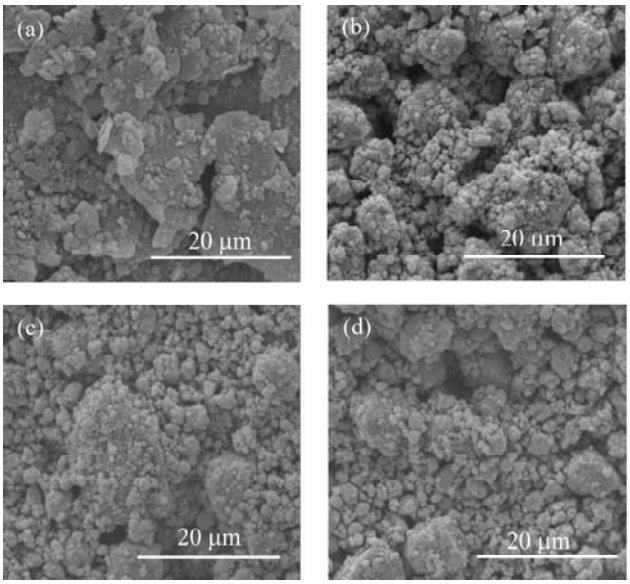

Figure 3. SEM micrographs of the powder after (a) 2 (b) 6 (c) 20 (d) 40-hours of milling

The internal structure of the reaction milled and annealed powder were investigated by the TEM. Figure 4 shows the bright field TEM micrograph and the corresponding selected area diffraction (SAD) pattern of 40-hours milled powder. Overall, the powder particle sample consists of wide size distribution, particle sizes ranging from 100 to 300 nm. The SAD shows ring patterns. Analysis of these ring patterns is difficult because different rings are not sharp and clear. The EDS spectrum shows the peaks of Fe, C and O. The presence of O_2 is due to oxidation of particles during milling.

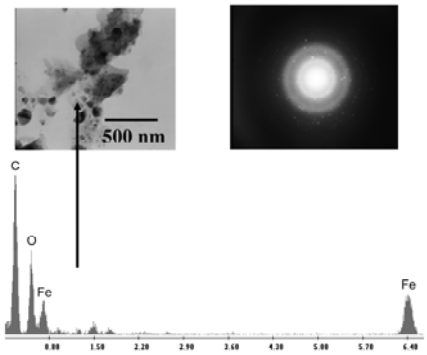

Figure 4. Bright field TEM micrograph and corresponding selected area diffraction (SAD) pattern of 40-hours milled powder. The EDS spectrum of particle is also shown in the Figure

Figure 5 shows the bright field TEM micrograph and the corresponding SAD pattern of 40-hours milled powder annealed at 600°C for 1 hour. The micrograph shows that particles are agglomerated and there is a growth of particles after annealing. The SAD shows ring pattern. The analysis of the ring pattern is in agreement with the XRD results.

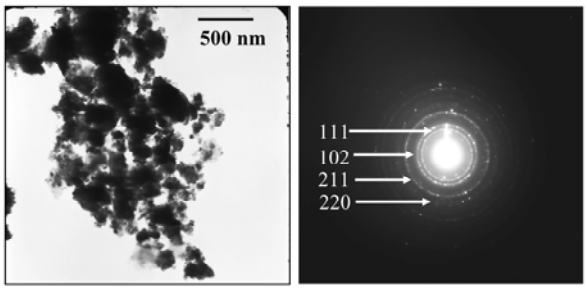

Figure 5. Bright field TEM micrograph and corresponding SAD pattern of 40-hours milled powder annealed at 600°C for 1 hour

The crystal size and lattice strain of the milled powder was determined from broadening of XRD peaks (Table 1). For this purpose, the as received as well as the milled powders were analyzed using x-ray diffraction (XRD) methods with CrK_{α} radiation. A correction for instrumental broadening was done. Broadening due grain size reduction and lattice strain accumulation were also separated (Chaira 2008 et al.).

Characterization of Silicon Carbide Powder

In order to determine the phase change of the powder mixtures during the reaction milling process, a small sample of milled product was repeatedly picked up at regular intervals for X-ray diffraction analysis. Figure 6 shows the XRD graph of powder milled for 40-hours. The two different X-ray patterns correspond to milled powder prepared by using 6 and 12 mm diameter steel balls. In either spectrum the peaks corresponding to Si_5C_3, SiC and βSiC are present. However, the intensity of silicon carbide

Table 1. Crystal size and lattice strain measured from XRD peaks

Milling time (h.)	Crystal size (nm)		Lattice strain
	Fe	Fe_3C	
Original	66		0
10 hours	31		$5.80*10^{-3}$
20 hours	15		$6.75*10^{-3}$
40 hours		4	$8.11*10^{-3}$
Annealed, 600°C, 1 h		29	
Annealed, 700°C, 1 h		40	

peaks is higher corresponding to the powder that was processed with 12 mm diameter steel balls as compared to the powder processed by 6 mm balls under identical conditions. At the end of the experiment, it was also observed that the 6 mm balls were invariably found coated with the powder whereas no such coating was observed on the 12 mm balls. This shows that the intensity of impact in case of 12 mm diameter ball is sufficient to dislodge any coating that forms on the surface of the ball.

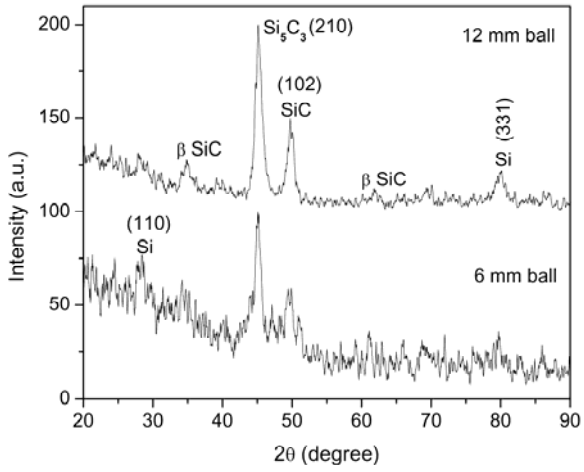

Figure 6. XRD patterns of milled powder at 40-hours of milling times for two different size balls (Cu target).

The XRD patterns of the end product (as milled SiC powder) are shown in Fig. 7 for different intervals of milling time. Several interesting observations are made. First, the graphite peak disappeared after about 10 hours of milling. This is a general observation in this study, which may be due to the amorphization of graphite during milling. However, at this stage the disappearance of the graphite peaks was not accompanied by a shift in the silicon peaks. As Si structure is more open structure (as compared to Fe), so C can be more easily accommodated in Si without much change in lattice parameter. Second, with increased milling time, silicon peaks also disappeared and silicon carbide peaks were observed. The silicon peaks disappeared around 20 hours of milling. Finally, as evident from Fig. 7, the Bragg peaks for the milled product (after about 40 hours of milling) are broad, suggesting accumulation of lattice strain and reduction in crystallite size. These two individual contributions to broadening have been analyzed in the next section. In comparison, El-Eskandarany *et al.* (1995) prepared stoichiomatric SiC powder by solid-state reaction of elemental silicon and carbon powder via the room temperature mechanical alloying process. Complete fcc–SiC alloy powder was obtained after 300-hours of milling.

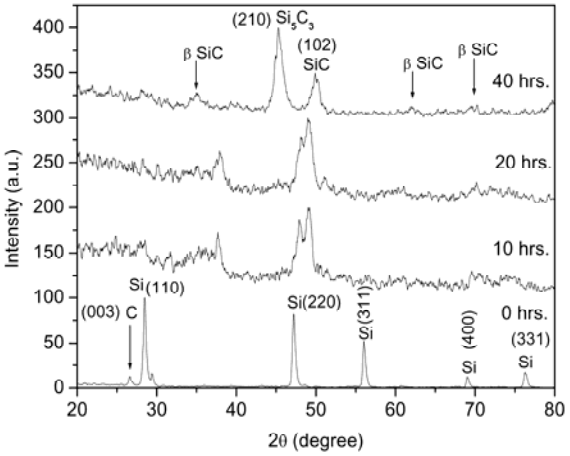

Figure 7. XRD patterns of milled powder at selected milling times using 12 mm diameter ball (Cu target)

The decrease of the grain size and introduction of lattice strain, which characterizes the activation process, has been determined using the X-ray diffraction patterns. Although the accumulation of lattice strain is a measure of defect formation, determining the defect structure is a more difficult task. The crystallite size and the lattice strain of the powder measured from the XRD peak broadening is shown as a function of milling time in Fig. 8. It can be seen that the crystallite size decreases and the internal strain increases rapidly with milling time up to about 20 hours. With further milling the crystallite size remains almost constant but internal strain appears to decrease. This could be attributed to the onset of phase change (i.e., nucleation of SiC). Finally, from Fig. 8 it is noticed that the different mass of the balls results in different crystal size and strain accumulation rates.

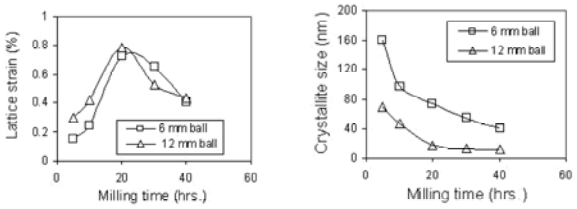

Figure 8. Effect of ball size on lattice strain and the crystallite size of the milled powder calculated from X-ray diffraction patterns; left: lattice strain; right: crystal size

The SEM technique was used to follow the changes in shape and size of the milled powder during the different stages of the reaction milling process. Figure 9 shows the SEM micrographs of the milled powder after different intervals of milling time. All the micrographs are of the same magnification. At the initial

stage of milling, the powder of the reactant materials is bulky, with random shape and size. As the milling progressed the powder became rounded as evident from Fig. 9 (d), which corresponds to 40-hours of milling. It is also evident from the SEM images that the particle size decreases gradually with increasing milling time. However, in contrast to milling of Fe-C powders, no evidence of particle coarsening could be observed in SEM.

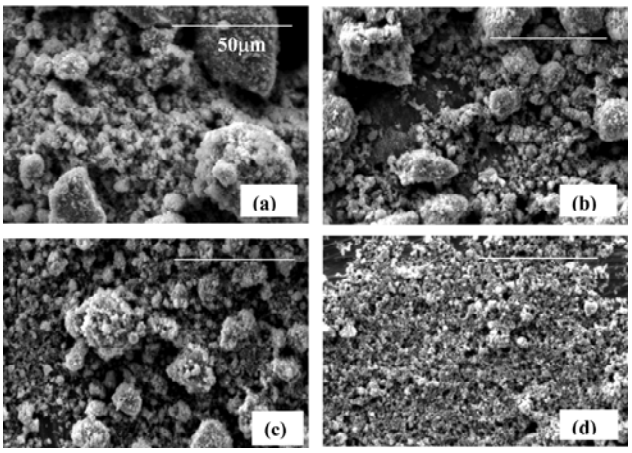

Figure 9. SEM micrographs of the powder after (a) 10 (b) 20 (c) 30 and (d) 40-hours of milling

To reveal more information, the internal structure of the reaction milled 40-hours powder was investigated by the TEM technique. This technique provides information on the structure of the powder particles. Figure 10 shows the bright field TEM micrograph and corresponding SAD pattern of 40-hours milled powder. The micrograph shows a wide size distribution of particles ranging from 300 nm to 500 nm. The EDS spectrum shows the peaks of Si, C and Fe. Due to contamination, Fe comes from jar surface and steel balls during milling. Since XRD shows no Fe peak, it is concluded that Fe contamination is small. Indexing of the diffraction pattern (Fig. 10) showed that the patterns are Si_5C_3.

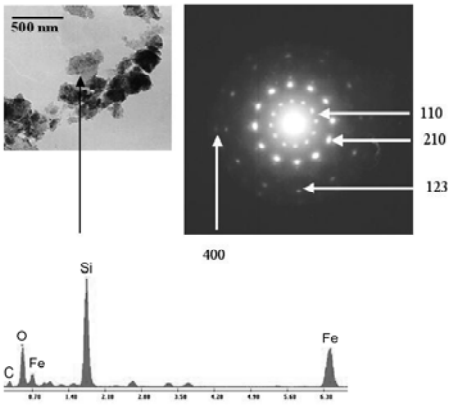

Figure 10. Bright field TEM micrograph and corresponding SAD pattern. The EDS spectrum of a particle is also shown in the Figure

Characterization of Titanium Carbide Powder

Reaction milling of Ti and C powders was done using pure graphite and activated carbon. This was because a number of studies in literatures have used both graphite and activated carbon as carbonaceous materials. Figure 11 shows the XRD patterns of powder milled for 10 hours. The two different XRD patterns correspond to the powder prepared by milling Ti with graphite and Ti with activated carbon powder separately. In both cases the X-ray diffraction pattern shows formation of TiC and peaks have similar intensities. From practical standpoint it was realized that pure graphite is a dry lubricant and could act as a lubricant during milling. This in turn slows or hinders the milling process. Therefore all the milling experiments have been restricted to activated carbon/titanium system.

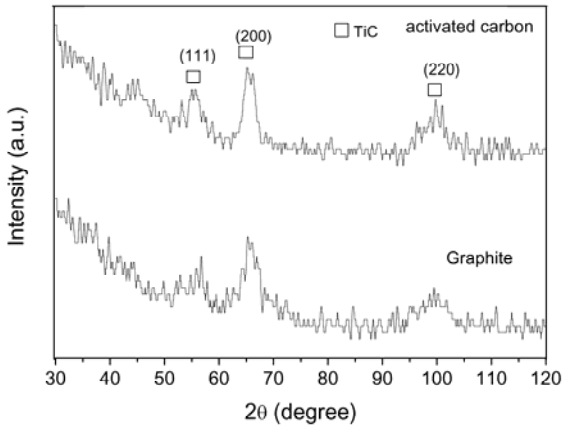

Figure 11. XRD patterns of powder milled Ti with graphite and Ti with activated carbon for 10 hours (Cr target)

Figure 12 shows the XRD patterns of Ti and activated carbon powder milled for different periods. XRD pattern shows that after 5 hours of milling almost all Ti peaks disappeared and peaks of TiC appeared. The graph shows the peaks of TiC, which were found after 10 hours of milling. After 10-hours of milling, peaks are broad, which indicates strain accumulation and grain refinement. In comparison, it is reported in the literature by Tang *et al.* (2006) who also synthesized $Ti_{50}C_{50}$ powder by mechanical alloying from elemental Ti and graphite powder that it is possible to synthesize TiC powder by mechanical alloying by 80 hours. It was observed that a solid solution of C in Ti, Ti(C), was first formed, followed by TiC. After milling for 80 hours, the powder was composed of TiC with grain size of 6 nm and a small amount of Ti(C) that was finally completely transformed to TiC after heat treatment.

Crystal size and lattice strain of the milled powder were determined from the broadening of XRD peaks. For this purposes, as received as well as the milled powder were analyzed using X-ray diffraction (XRD) methods with CrK_α radiation. The crystallite size and the lattice strain of the powder measured from the XRD peak broadening is shown in Table 2. After 10 hours of milling, crystal size of TiC was found to be 3 nm. The Table also shows that lattice strain increases with milling.

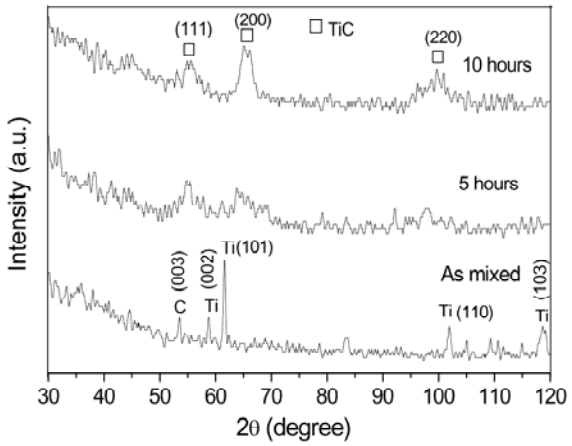

Figure 12. XRD patterns of powder milled for 10 hours, using activated carbon as a starting carbon material (Cr target)

Table 2. Crystal size & lattice strain measured from XRD peaks

Milling time (hours)	Crystal size (nm)		Lattice strain	
	Ti + activated carbon	Ti + graphite	Ti + activated carbon	Ti + graphite
0	79	98	0	0
5	12	20	$3.82*10^{-3}$	$5.03*10^{-3}$
10	3	2	$5.36*10^{-3}$	$7.25*10^{-3}$

SEM was used to study the changes in shape and size of the milled powder during different stages of the reaction milling process. Figure13 shows the SEM micrographs of the milled powder after selected times for Ti+activated carbon and Ti+graphite system. For Ti+activated carbon system, the powder of the reactant materials of Ti and C was bulky, with random shape and size. During early stages of milling (2 hours) the powder tends to agglomerate and deform and as a result large flakes were formed. The powder particles undergo cold welding by binding to each other under stress and further deform resulting in flaky particles. After 5 hours of milling, the flakes thin down under stress and larger agglomerates were formed. After 10-hours of milling, large agglomerates were disintegrated into smaller powder with an average diameter of 1-2 μm. The SEM micrographs of Ti+graphite also show same morphology like Ti/activated carbon system. The only difference here is that the powder particles are still flaky after 5 hours grinding.

TEM of the milled Ti+activated carbon powder was carried out to get actual size of the powder particles. Figure 14 shows the bright field TEM micrograph and corresponding selected area diffraction pattern (SADP). The micrograph shows that milled powder is fine and fog-like, and particle sizes are in the range of 100-200 nm. The SAD shows ring pattern. The different diffraction rings refer to (111), (200), (220) and (311) planes of the fcc TiC, respectively, which correspond to the XRD results shown earlier. The absence of the spots in the SADP indicates the formation of fine grain TiC powder.

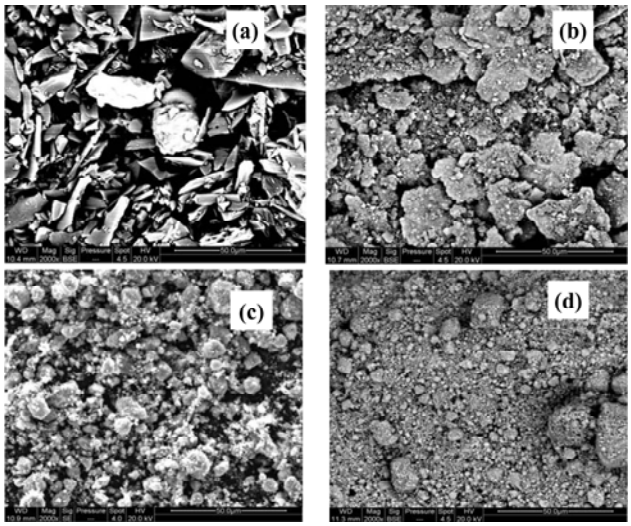

Figure 13. SEM micrographs of Ti and activated carbon powder after 0, 2, 5 and 10 hours of milling

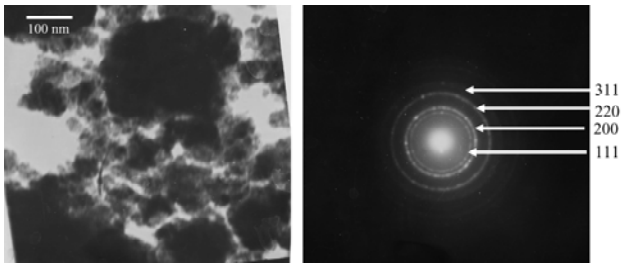

Figure 14. Bright field (BF) TEM micrograph and corresponding selected area diffraction pattern (SADP)

Conclusions

It is possible to prepare nanocrystalline carbides from elemental powders in dual drive planetary mill by reaction milling. Forty hours milling time is required to prepare nanocrystalline cementite and silicon carbide powder, whereas only 10 hours is required to prepare titanium carbide. Preliminary investigations on bulk carbide synthesis which is the main focus of the work showed promising results that support the need for further research to address the contamination and scale-up issues. Although synthesis of carbides have been shown in smaller ball mills, the present concept of engineering the process in the dual drive planetary mill makes the process innovative. More important, it leads one to believe that some of the industrially important carbides can be produced by reaction milling at industrial scale. There is plenty of scope for improved design of the milling system with enhanced energy efficiency to make reaction milling a viable commercial technique for bulk carbide production.

References

1. L.L. Ye, and M.X. Quan, 1995, Synthesis of nanocrystalline TiC powders by mechanical alloying, *Nanostructured Materials,* 5(1) (1995) 25-31.
2. R.K. Rajamani, L. Milin, and G. Howell, G., Dual drive planetary mill, US Patent 6,086,242, 2000.

3. D. Chaira, B.K. Mishra and S. Sangal, Synthesis and characterization of silicon carbide by reaction milling in a dual-drive planetary mill, *Materials Science & Engineering A,* 460-461 (2007) 111-120.
4. M. Umemoto, Y. Todaka, T. Takahashi, P. Li, R. Tokumiya, K. Tsuchiya, High temperature deformation behavior of bulk cementite produced by mechanical alloying and spark plasma sintering, *Materials Science & Engineering A,* 375-377 (2004) 894-898.
5. G.W. Wang, S.J. Campbell, A. Calka, W.A. Kaczmarek, Ball-Milling of Fe-C (20-75% Fe), *Nanostructured Materials,* 6 (1995) 389-392.
6. D. Chaira, S. Sangal and B.K. Mishra, Efficient synthesis and characterization of iron carbide powder by reaction milling, *Powder Technology,* 191(1-2) (2009) 149-154.
7. M.S. El-Eskandarany, K. Sumiyama, and K. Suzuki, Mechanical solid state reaction for synthesis of β-SiC powders, *Journal of Materials Research,* 10(3) (1995) 659-667.
8. W.M. Tang, Z.X. Zheng, W.C. Wu, J. Lu, J.W. Liu, and J.M. Wang, Structural evolutions of mechanically alloyed and heat treated $Ti_{50}C_{50}$ and $Ti_{33}C_{67}$ powders, *Materials Chemistry and Physics,* 99 (2006) 144-149.